



Article

Dynamics of Forest Vegetation in an Urban Agglomeration Based on Landsat Remote Sensing Data for the Period 1990–2022: A Case Study

Elena Petrovna Yankovich ¹, Ksenia Stanislavovna Yankovich ² and Nikolay Viktorovich Baranovskiy ^{3,*}

¹ School of Earth Sciences & Engineering, Tomsk Polytechnic University, 634050 Tomsk, Russia; yankovich@tpu.ru

² Partenor Digital Tour Initiale, 75008 Paris, France

³ School of Energy & Power Engineering, Tomsk Polytechnic University, 634050 Tomsk, Russia

* Correspondence: firedanger@yandex.ru

Abstract: In recent years, the vegetation cover in urban agglomerations has been changing very rapidly due to technogenic influence. Satellite images play a huge role in studying the dynamics of forest vegetation. Special programs are used to process satellite images. The purpose of the study is to analyze forest vegetation within the territory of the Tomsk agglomeration based on Landsat remote sensing data for the period from 1990 to 2022. The novelty of the study is explained by the development of a unique program code for the analysis of Landsat satellite data on the previously unexplored territory of the Tomsk agglomeration with the prospect of moving to the scale of the entire state in the future. In this study, the authors present an algorithm implemented in Python to quantify the change in the area of vegetation in an urban agglomeration using Landsat multispectral data. The tool allows you to read space images, calculate spectral indices (NDVI, UI, NDWI), and perform statistical processing of interpretation results. The created tool was applied to study the dynamics of vegetation within the Tomsk urban agglomeration during the period 1990–2022. Key findings and conclusions: (1) The non-forest areas increased from 1990 to 1999 and from 2013 to 2022. It is very likely that this is due to the deterioration of the standard of living in the country during these periods. The first time interval corresponds to the post-Soviet period and the devastation in the economy in the 1990s. The second period corresponds to the implementation and strengthening of sanctions pressure on the Russian Federation. (2) The area of territories inhabited by people has been steadily falling since 1990. This is due to the destruction of collective agriculture in the Russian Federation and the outflow of the population from the surrounding rural settlements to Tomsk and Seversk.

Keywords: remote sensing data; forest vegetation; urban agglomeration; Landsat; Python; NDVI; UI; NDWI; Tomsk



Citation: Yankovich, E.P.; Yankovich, K.S.; Baranovskiy, N.V. Dynamics of Forest Vegetation in an Urban Agglomeration Based on Landsat Remote Sensing Data for the Period 1990–2022: A Case Study. *Remote Sens.* **2023**, *15*, 1935. <https://doi.org/10.3390/rs15071935>

Academic Editors: Alfredo Huete, Junxiang Li, Conghe Song, Tao Lin, Hong Ye and Guoqin Zhang

Received: 14 January 2023

Revised: 8 February 2023

Accepted: 29 March 2023

Published: 4 April 2023



Copyright: © 2023 by the authors. Licensee MDPI, Basel, Switzerland. This article is an open access article distributed under the terms and conditions of the Creative Commons Attribution (CC BY) license (<https://creativecommons.org/licenses/by/4.0/>).

1. Introduction

Urbanization of territories around the world leads to an increase in the environmental impact on vegetation [1–4]. Forests are within the city limits, which leads to changes in forest vegetation [5–7]. Understanding and knowledge of where these changes occur, in what quantity and under the influence of what factors are important for assessing the quality of the environment and determining management decisions to ensure the hygienic and environmental safety of the population [8–10].

Satellite images play a huge role in studying the dynamics of forest vegetation [11–15]. They allow us to obtain objective information about spatial and temporal changes in vegetation. Multispectral space images from Landsat satellites are the most suitable type of remote sensing data for the analysis of dynamic changes at the regional level [16]. A characteristic feature of the Landsat program is the inheritance of the spectral ranges in which the survey is carried out, which ensures the continuity and compatibility of

data obtained by different satellites of the Landsat series during the entire period of the program [17–20].

There are various methods for detecting areas occupied by vegetation. They include both visual interpretation and automatic image processing, including supervised and unsupervised classification, and the creation of index images. An analysis of vegetation cover dynamics can be carried out using vegetation indices obtained from time images [21].

Processing of satellite images is usually carried out using special programs [22–24]. These programs can be divided into two groups. The first group is universal systems that allow us to solve many problems of analyzing data from remote sensing of the Earth. The second group comprises programs (tools) developed to solve highly specialized tasks. The undoubted advantage of such programs is that they are created to solve a specific practical problem. Most of the steps in such programs are automated. After analyzing the existing solutions regarding the goal of the study, it was decided to create a tool for assessing vegetation changes within an urban agglomeration based on multi-temporal images.

In the work, an algorithm for analyzing satellite images was developed, implemented in the Python language [25], which facilitates reading satellite images, calculating spectral indices, calculating the cloudiness mask, and performing statistical processing of the interpretation results. The tool performs a classification of multi-temporal images to determine the dynamics of areas occupied by vegetation.

The purpose of the study is to analyze forest vegetation within the territory of the Tomsk agglomeration using Landsat remote sensing data for the period from 1990 to 2022. Main research objectives: (1) Preparation of the database of Landsat satellite images for the period from 1990 to 2022; (2) Development of an algorithm and software implementation based on the high-level programming language Python; (3) Spatio-temporal analysis of the territory of the Tomsk agglomeration and the marking out of forested areas, urban areas and areas not classified as forested; (4) The formulation of the main mechanisms that led to the identified changes in the forest areas of the Tomsk agglomeration.

The novelty of the presented scientific research is explained by the development of a unique Python code for the analysis of Landsat remote sensing data on the territory of the Tomsk agglomeration. This is a pilot study conducted in the Western Siberia region. Previously, such studies on changes in forest cover were not carried out in the Tomsk region in the context of changes in the social, economic and political situation in the Russian Federation. The position of novelty should be explained in more detail. Developing our own program code opens up prospects for its wide practical application. As known, in the Russian Federation, there is an Information system for remote monitoring of forest fires, named ISDM-Rosleskhoz. The main purpose of this system is to monitor, assess and predict forest fire danger across the territory of the Russian Federation.

The operation of this system is provided by the federal state institution Aviale-sookhrana. The developer of the program modules is the Center for Problems of Ecology and Forest Productivity of the Russian Academy of Sciences. This center conducts a wide range of research on forest ecology, including in cooperation with the Space Research Institute of the Russian Academy of Sciences. Possible interaction with this center opens up prospects for the introduction of new modules for assessing urban agglomerations, both in the context of environmental challenges and forest fire danger. It is known that cities and rural settlements are sources of anthropogenic pressure on adjacent forested areas. Industrial facilities have the same effect on forested areas. Therefore, the development of a unique program code opens up prospects for improving the functionality of ISDM-Rosleskhoz.

2. Background

Landsat images are the most used source of Earth remote sensing data for a wide range of studies [26–42]. The advantage of Landsat data is associated with the continuity of observations over 50 years and the policy of free access to images [27,28]. Today, users have access to the processed Landsat Collection 2 data. The main feature of Collection 2 is a significant improvement in the absolute geolocation accuracy of the global

ground reference dataset, which improves the compatibility of the Landsat archive over time. Collection 2 also includes updated global DEM sources, as well as calibration and validation updates [29,30]. Collection-based processing is important for the consistency of preprocessed data required for time series analysis. The introduction of Landsat collection processing has facilitated a shift in the use of Landsat data from single imagery to time series analysis. Thus, one of the problems of limiting the use of Landsat data time series associated with the need for preliminary geometric correction was solved. However, a number of limitations remain associated with the uneven geographical and temporal coverage of the regions of the world by Landsat data for environmental, technical and programmatic reasons. The Landsat swath ensures that the survey of one area is repeated once every 16 days. Seasonality and cloud cover also reduce the viability of annual land cover renewals [28,30]. The spatial resolution of Landsat images also has serious limitations in areas with high spatial heterogeneity [6].

Despite the above limitations, Landsat data are unique data for monitoring urban areas [43–51]. Monitoring is carried out using a wide range of Landsat input data analysis methods [26,28,45,47–54]. Land cover information is extracted from satellite images using various image analysis methods that have been developed in the field of remote sensing [40,43–45].

Mapping urban areas based on Landsat has a number of difficulties. Pixels of Landsat images of urban areas usually contain mixed information about anthropogenic objects and vegetation. Vegetation cover must be further extracted from the image when identifying urban areas. Urbanized territories do not have unique spectral characteristics, and when they are identified, there is considerable confusion with non-urban classes (for example, with “bare” soils) [47].

The works [26,45,47–54] consider methods for classifying urbanized territories. Let us focus on those that are of interest to us. One approach involves using spectral indices such as normalized difference vegetation index and normalized building index to separate urban from non-urban lands [48,50]. Another spectral approach [24] assumes that urban pixels consist of linear combinations of three common components of land cover, vegetation, impervious surface and soil (the so-called V–I–S model). Mapping of the urban area to be carried out with a combination of spectral and spatial information is proposed in the work of Guindon et al. [47]. The method consists of the following two independent classifications based on pixels and based on segments (segment based) of elementary coverage classes. They are then combined using rules that allow the class legend to be augmented by inferring additional land use classes based on spatial context and automatically edited to reduce classification errors due to spectral confusion between classes.

3. Materials

3.1. Study Area

The Tomsk agglomeration is one of the largest urban agglomerations in the Siberian Federal District of Russia. The Tomsk agglomeration is formed around the administrative center of the Tomsk region—the city of Tomsk (Figure 1). According to the draft “Schemes of territorial planning of the Tomsk region” [55], Tomsk agglomeration includes the Tomsk urban district, ZATO Seversk, Tomsk district, the western part of the Asinovsky district (Asinovskoye urban settlement, Novikovskoye, Yagodnoye, Bolshedorohovskoye rural settlements), the eastern part of the Shegarsky district (Shegarskoye and Pobedinskoye rural settlements) and the northeastern part of the Kozhevnikovskiy district (Kozhevnikovskoe rural settlement) (Table 1).

Within the boundaries of the study area, there are two large cities of Tomsk and Seversk, and a number of small settlements with a total population of more than 800 thousand people. In the valleys of the Ob and Tom rivers, the main number of rural settlements and recreational areas are concentrated.

The Tomsk agglomeration is located in the taiga zone (subzone of small-leaved forests), and only the extreme south is included in the forest-steppe zone with a humid climate [56,57].

According to the amount of precipitation, the region belongs to the zone of moderate moisture. The average annual precipitation ranges from 450–650 mm, which exceeds evaporation by 100–170 mm. The average annual air temperature for a long period is 0.4 °C.

The relief is flat, flat with a slight slope from south to north (the minimum absolute marks are 65–75 m, the maximum are 200 m).

Table 1. Composition of the agglomeration.

Municipality Name	Territory km ²	Population 1 January 2016
Tomsk	297.20	590,826
Seversk	485.65	114,549
Tomsk area	10,035.22	72,386
West part of Asinovskoe area:		
Asino	89.85	24,615
Bolshedorohovo	249.97	950
Novikovskoe	272.93	1308
Yagodnoe	297.00	1394
Northern East part of Kozhevnikovo area:		
Kozhevnikovo	397.12	8351
East part of Shegarskiy area:		
Pobeda	223.41	2134
Shegarskoe	202.30	8789
Total agglomeration	12,550.65	825,302
Part of Tomsk region	3.96%	76.65%

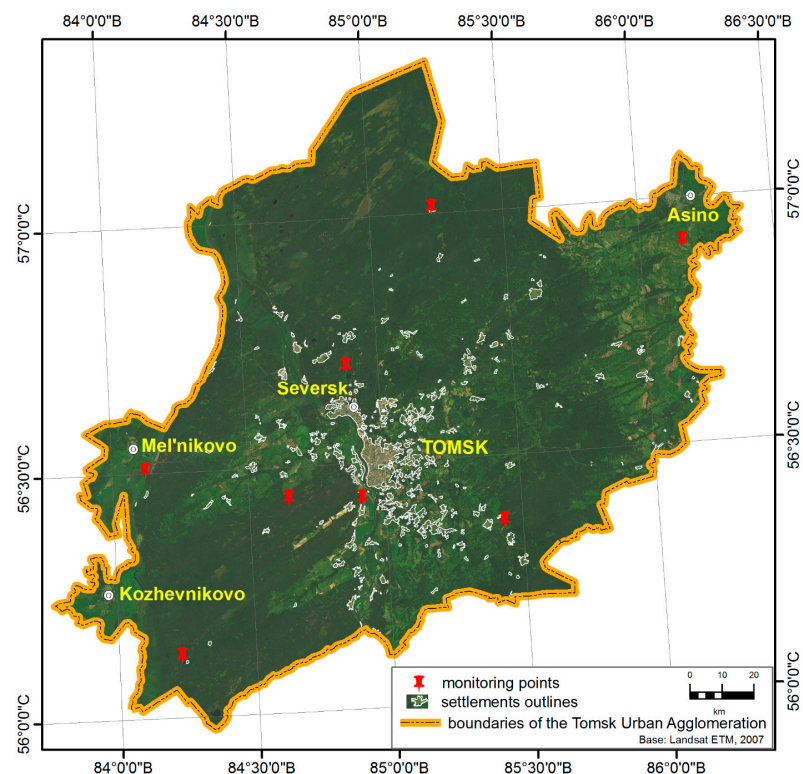


Figure 1. The study area of Tomsk agglomeration.

3.2. Data

In this work, remote sensing data obtained from Landsat satellites were used. Archival images from the optical sensors of the Landsat L2 C2 products from 1990 to 2022 with low cloudiness were downloaded from the online service of the US Geological Survey (USGS) website [58] (Table 2). Data from Landsat-5 (TM), Landsat-7 (ETM+) and Landsat-8 (OLI) satellites for the summer phenological period were used to study the dynamics of the area of forest vegetation in the study area. The selected area is covered by several scenes. To highlight the area of interest, a vector shapefile of territory boundaries was used.

Table 2. List of satellite image.

ID	Name	Date	Satellite	Cloud Cover, %	Path/Row
1	LT05_L2SP_148020_19890626_20201008_02_T1	26 June 1989	LANDSAT_5	1.0	148/20
2	LT05_L2SP_148021_19900613_20200915_02_T1	13 June 1990	LANDSAT_5	2.0	148/21
3	LE07_L2SP_147020_19990709_20200918_02_T1	9 July 1999	LANDSAT_7	0.0	147/20
4	LE07_L2SP_147021_19990709_20200918_02_T1	9 July 1999	LANDSAT_7	0.0	147/21
5	LE07_L2SP_149020_19990707_20200918_02_T1	7 July 1999	LANDSAT_7	0.0	149/20
6	LE07_L2SP_149021_19990707_20200918_02_T1	7 July 1999	LANDSAT_7	0.0	149/21
7	LT05_L2SP_148020_20070714_20200830_02_T1	14 July 2007	LANDSAT_5	0.0	148/20
8	LT05_L2SP_148021_20070714_20200830_02_T1	14 July 2007	LANDSAT_5	0.0	148/21
9	LC08_L2SP_148020_20130714_20200912_02_T1	14 July 2013	LANDSAT_8	0.9	148/20
10	LC08_L2SP_148021_20130714_20200912_02_T1	14 July 2013	LANDSAT_8	0.01	148/21
11	LC08_L2SP_148020_20200818_20200823_02_T1	18 August 2020	LANDSAT_8	5.1	148/20
12	LC08_L2SP_148021_20200802_20200914_02_T1	2 August 2020	LANDSAT_8	0.09	148/21
13	LC09_L2SP_148020_20220613_20220615_02_T1	13 June 2022	LANDSAT_9	1.74	148/20
14	LC08_L2SP_149021_20220612_20220617_02_T1	12 June 2022	LANDSAT_8	9.88	149/21
15	LC09_L2SP_147021_20220809_20220811_02_T1	9 August 2022	LANDSAT_9	1.2	147/21

The work utilizes 5 bands (Blue, Red, Green, Near Infrared and Short Wave Infrared), which have spatial definition of 30 m (Table 3).

Table 3. The 30 m Spatial Resolution Bands.

Band	Landsat 5 TM	LANDSAT 7 ETM+	Landsat 8/9 OLI
	Band number: Wavelength	Band number: Wavelength	Band number: Wavelength
Blue	Band 1: 0.45–0.52	Band 1: 0.45–0.52	Band 2: 0.45–0.51
Green	Band 2: 0.52–0.60	Band 2: 0.52–0.60	Band 3: 0.53–0.59
Red	Band 3: 0.63–0.69	Band 3: 0.63–0.69	Band 4: 0.64–0.67
Near Infrared	Band 4: 0.76–0.90	Band 4: 0.77–0.90	Band 5: 0.85–0.88
SWIR 2	Band 7: 2.08–2.35	Band 7: 2.08–2.35	Band 7: 2.11–2.29

3.3. Spectral Indexes

Combinations of spectral bands of images provide information about the Earth's surface. Below is a brief description of the spectral indices used in this work. The Normalized Differential Vegetation Index (NDVI) indicates the presence and condition of vegetation and is widely used for vegetation mapping [59]. The construction of the index is based on the fact that the chlorophyll of plant leaves reflects radiation in the near infrared range of the electromagnetic spectrum and absorbs in the red [60,61]. Thus, the presence of vegetation in each pixel of the image is determined by the difference between the intensities of the reflected light in the infrared and red ranges, divided by the sum of their intensities (1). The

ratio of the brightness values in these two channels allows you to separate the vegetation from other objects. The range of NDVI values varies from -1 to 1 ; for vegetation, the NDVI index takes on positive values.

$$\text{NDVI} = (\text{NIR} - \text{RED}) / (\text{NIR} + \text{RED}), \quad (1)$$

where NIR is the value of pixels in the near infrared region of the spectrum; RED—value of pixels in the red region of the spectrum.

The open water surface can be determined based on the fact that water reflects much less light in the infrared than in the visible [62]. The input features are well defined by the values of the normalized difference water index (NDWI). NDWI was calculated using the formula proposed in [63]:

$$\text{NDWI} = (\text{Green} - \text{NIR}) / (\text{Green} + \text{NIR}), \quad (2)$$

where NIR is near infrared, and Green is reflection in the green region of the spectrum.

The Urban Index (UI) [64–66] was used to interpret urban areas. The index uses NIR and SWIR2 (near infrared and shortwave infrared) channels to highlight built-up areas. This factor allows you to muffle the difference in surface illumination, as well as atmospheric effects.

$$\text{UI} = (\text{SWIR2} - \text{NIR}) / (\text{SWIR2} + \text{NIR}), \quad (3)$$

where SWIR2 is shortwave infrared, and NIR is near infrared.

The question of algorithm validation always arises when proprietary software is used. It should be noted that the developed script performs image analysis using well-known and proven formulas for calculating spectral indices. Such formulas are standard, they are used in many works and their additional verification is not required. However, in 2022, ground-based observations were carried out on the territory of the Tomsk agglomeration in order to compare image processing data and actually recorded conditions in a specific area at the monitoring point. The location of the control points is shown in Figure 1. In subsequent years, an annual analysis of field observation data and the results of the developed script will be carried out. We emphasize that the script uses well-known verified formulas for calculating spectral indices.

4. Methods

The general research methodology is shown in Figure 2. Previously, images in the GeoTIFF format of the Landsat satellite system for the specified time period are downloaded from the site, and cloudiness is less than 5%. A database of temporary images of the territory is being formed. In addition to images for the study, it is required to prepare the boundaries of the study area in vector format to highlight the area of interest in the images.

ArcGIS is a complete system for working with data. The functionality of ArcGIS has been extended with Erdas Imagine modules, which allows you to perform complex analysis and image processing. However, like any paid software product, ArcGIS has limitations. To use the program, you must have an up-to-date ArcGIS license. Your computer hardware and operating system must meet the minimum requirements. These requirements are necessary to run the ArcGIS program for execution. The ArcGIS user does not have full access to the processing process and control over each step. In addition, the user must have extensive knowledge to take full advantage of the unique features and data analysis tools in ArcGIS. To solve the exploration problem, the user will need to build a solution model in ModelBuilder to run the workflow, or create a Python script outside of ArcGIS or in ArcGIS.

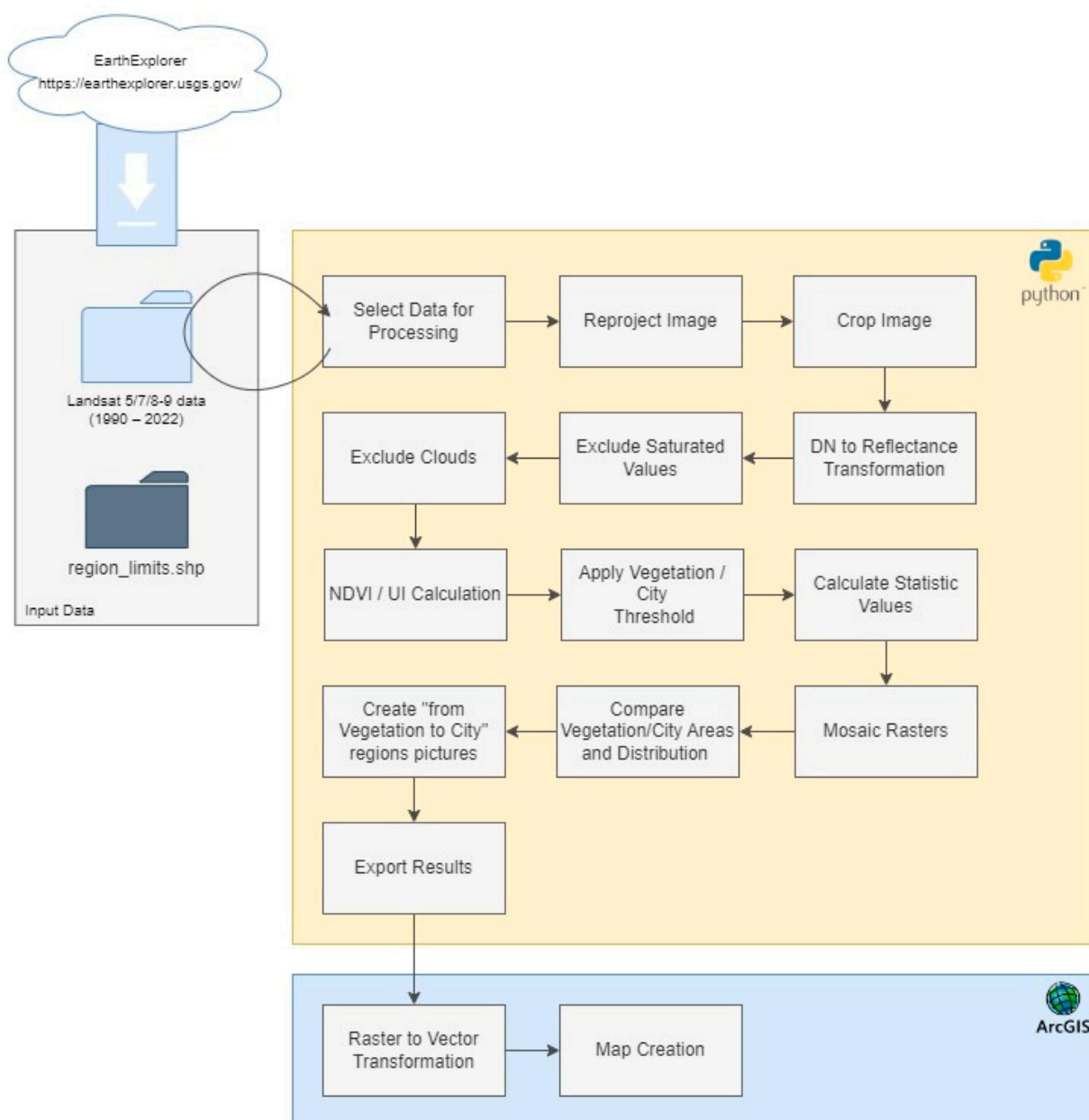


Figure 2. Flowchart of the research method.

The presented Python script was created to perform an analysis of the dynamics of vegetation change in urban areas based on the analysis of Landsat images in automatic mode and does not require any specialized knowledge from the user. The user's function is to run the script and provide input. The script can be run standalone on any computer and is independent of ArcGIS licenses and changes in new versions of the program. The next goal of updating the script is to add calculation of other spectral indices for Landsat images, perform Sentinel image processing and provide online access to the Script.

The imaging stage consists of processing all available datasets. Image pixel data presented in the dimensionless value DN are recalculated for digital processing of Landsat images into reflectance [67]. "Lighted" pixels and clouds with their shadows are excluded from processing. Raster images of various channels necessary for processing and calculation of indices are loaded into the program. Then, the images are cropped according to the area of interest, a mask is applied to the selected images in the shape-file format with territory boundaries. The study area is located at the intersection of images, so several scenes (from

2 to 4) are used for each time period. The scenes covering the area can be in different coordinate systems (WGS84 44N and WGS84 45N). Before forming a solid region of interest, the processed data are reprojected into WGS84 (EPSG:4326) and combined into a mosaic.

The next stage consists of vegetation identification based on the data prepared in the previous stages. The presence or absence of vegetation is determined by the values of the Normalized Difference Vegetation Index (NDVI). The range of index values is from -1 to 1 . For vegetation, the NDVI index takes positive values. In this work, we are interested in pixels in which the NDVI values are in the range from 0.2 to 0.7 .

For more accurate results, area masks were used (cloud mask—based on the QA_PIXEL.tif band provided in the raster set; water surface mask—based on the normalized NDWI water index). Indices are calculated for each selected period from 1990 to 2022. The calculation of the area occupied by vegetation and the city is made in the program and issued as a table of results. It is possible to export processing results to ArcGIS, convert raster data to vector data, and build thematic maps. The algorithm is implemented in Python using Rasterio, Fiona and Numpy libraries. The algorithm is built in such a way that it works with individual scenes. The operations described below apply to each scene and are performed sequentially until all have been processed. The channels of interest were selected in each scene based on the configuration file.

A script for searching and uploading images is included in the tool. The following input data were used to script processing, namely, folder address, year and area of interest (vector shapefile with borders). At the initial stage, the script is used to find the folders corresponding to the selected year. If there are two images, then there will be two folders. The metadata of each image were loaded. Definite satellite on which the survey was made is determined by the metadata (in our case, it is LANDSAT 5/LANDSAT 7/LANDSAT 8/LANDSAT 9). Date of shooting (year, month and day) were used. The script has the ability to work with data archives. The script is used to unzip the data and save it to a folder, and only then the metadata will be downloaded.

Next step is the procedure for creating a cloud mask and preparing band rasters for calculating spectral indices. In the folder of each multichannel image, the script is used to find an image for the cloud mask (*QA_PIXEL.tif), to read it, to crop it to the area of interest, and to reproject it at the final stage. At the output, binary raster with masked clouds (0—clouds; 1—everything else) has been obtained.

Bitmaps of the blue, green, red, near infrared, shortwave infrared channels are reprojected and clipped to the region of interest, and DN pixel values are converted to reflection values. At the output, our own new bitmap in reflectance values and new metadata for the multiband raster were obtained for each channel.

Next, the indices were calculated, and index maps for each scene were build. At the output, rasters with calculated indices NDVI, UI and NDWI were obtained (Figures 3 and 4).

Mapping of forest and urban areas is carried out using arithmetic operations. A map of man-made areas is built by combining images of the built-up area index (UI from -0.2 to 1), cloudiness mask, water index and bare soil index. The vegetation map is built using the NDVI index from 0.2 to 0.7 , the cloud mask, the water index and the built-up area index.

Data were merged after processing all the folders with images of each year. It was checked that the data source of all input images is the same. Separate scenes are combined into a mosaic to obtain an integral territory. For example, at the input, several rasters for the red channel were used. Then, one raster and new metadata (new projection, raster size) were obtained at the output. Results were written in binary rasters.

The following statistical values were calculated, namely, total area, area occupied by man-made objects and area occupied by vegetation. The necessary rasters were saved to files for building maps.

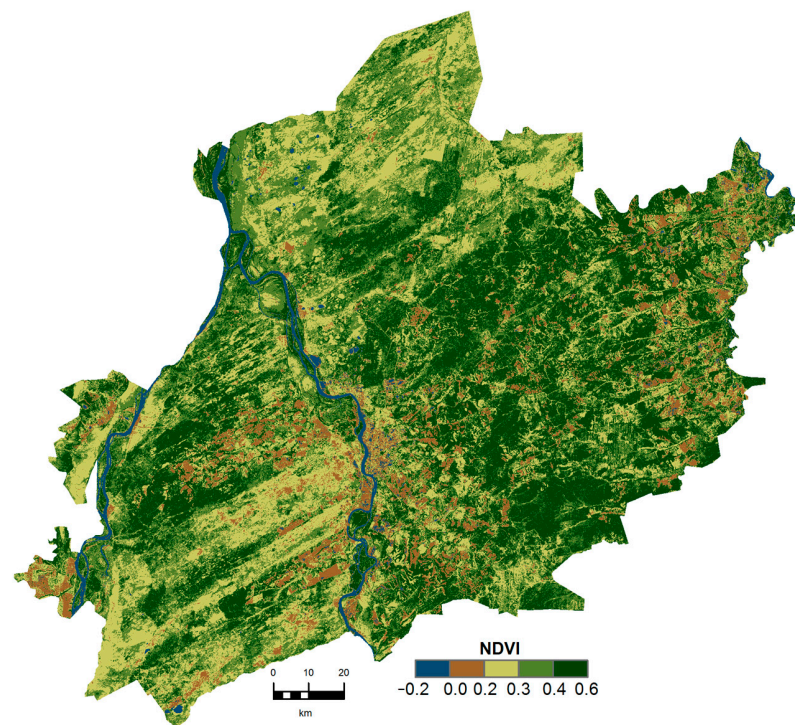


Figure 3. NDVI map.

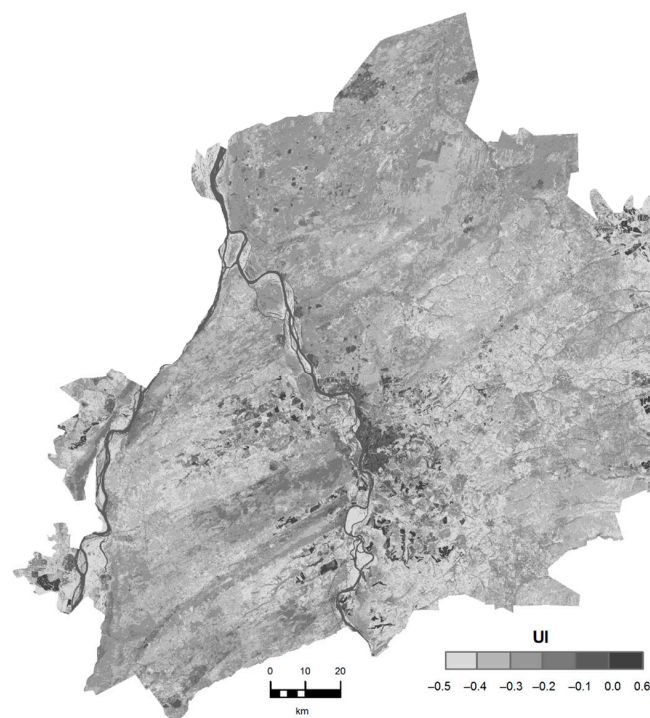


Figure 4. UI map.

5. Results and Discussion

A multi-index approach was applied to detect areas of occupied vegetation and built-up areas. At the first step, the images are selected and coordinated. Cropping images by the region of interest and combining them into mosaics allowed us to obtain all spectral bands and indices for the territory under consideration. The combination of binary rasters for vegetation and for the city area is shown in Figure 5.

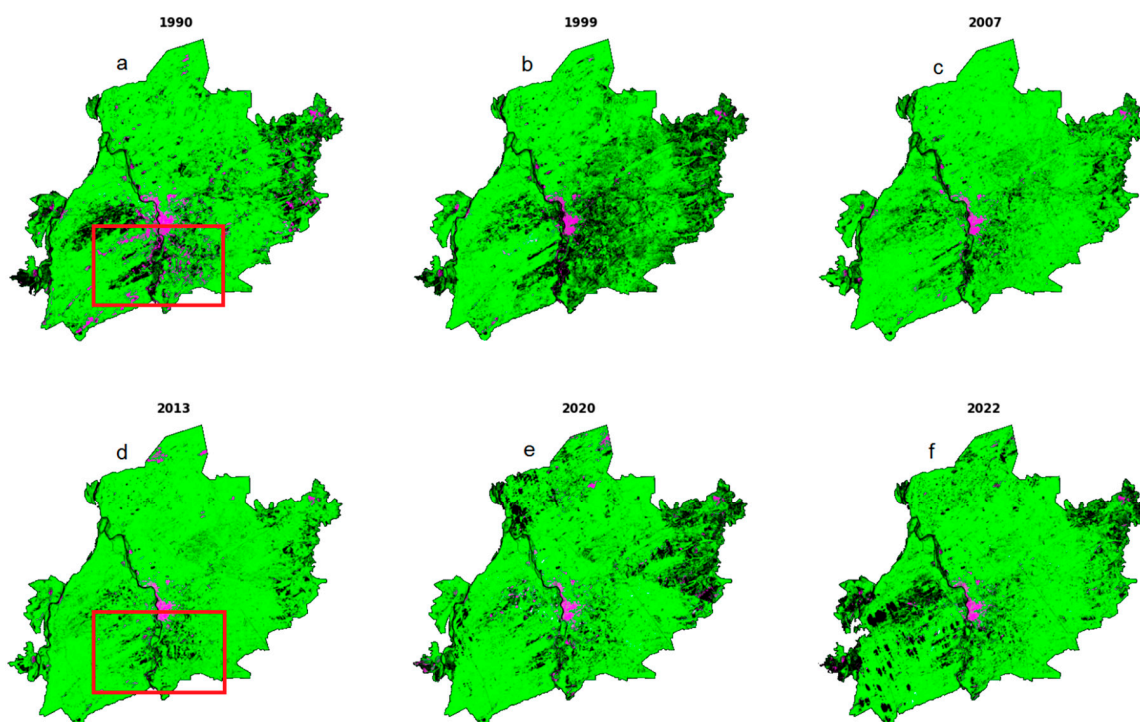


Figure 5. Mapping of forest vegetation in the Tomsk agglomeration. Legend: green for vegetation, purple for urban areas, black for other areas: (a)—1990 year; (b)—1999 year; (c)—2007 year; (d)—2013 year; (e)—2020 year; (f)—2022 year. Red box is maximum changes after initial state.

When using remote sensing data to assess wintering in the forest cover, different time steps can be used to evaluate satellite images. Often, a regular time grid is used with a step of 5 years. This is the correct approach to assessing changes in forest cover when assessing the impact of weather, climate, and successional processes within a biogeocenosis. However, in this work, this approach is not acceptable and is erroneous. It is necessary to use a heterogeneous grid over time with irregular time steps, chronologically linked to anchor points among social, economic and political events during the analysis of changes in forest cover in the context of social, economic and political impacts. The main reference points are presented in Table 4.

Table 4. Control points in chronological order.

N	Year	Event	Impact
1	1990	USSR was destroyed	Economical chaos in the Russian Federation
2	1999	Political elites transfer	New aims to stable situation in the Russian Federation
3	2007	All-Russian reformation of Forestry	Reduction in forest services, transfer of responsibilities from state to regional level
4	2013	Last stable year before sanctions against the Russian Federation	Sanctions led to economical problems in the Russian Federation
5	2020	COVID-19 Pandemic	Corruption of external connections with partners in the world, unemployment was increased
6	2022	Current time, new sanctions against the Russian Federation	Sanctions led to economical problems in the Russian Federation

It can be emphasized that the interval of 5 years is in no way connected with these events in the social, economic and political sphere of the country as a whole and the Tomsk agglomeration in particular.

Figure 6 shows the dynamics of vegetation change in the presented years. The algorithm makes it possible to identify forests, other territories and urban areas. It can be seen in Figure 5a that in 1990, there was an insignificant share of other territories in the Tomsk agglomeration. This period should be used as some initial reference. As is known, in 1990–1991, the destruction of the Soviet Union took place [68]. With the acquisition of independence in the Russian Federation in the 1990s came lawlessness and the destruction of all subsystems of the state, including forestry. These negative changes also affected the Tomsk agglomeration. Illegal logging and burning of forests began during this period. Moreover, no one removed the logging residues at the felling sites. The following figure, Figure 5b, shows a large number of areas that are not classified as a forest or urban area. In fact, these are scorched stands, cuttings and garbage dumps. Additionally, by 1999, these territories had reached the maximum area. At the end of 1999, in the Russian Federation, there was a change in the ruling elites under the leadership of the new president [69]. The country took a course towards improving the economic and social components of life. Figure 5c shows that forest fragmentation has significantly decreased in the Tomsk agglomeration. These processes continued until 2013 (Figure 5d). However, it was not possible to completely get rid of the fragmentation of forest tracts. This is probably due to the adoption of the new Forest Code of the Russian Federation [70]. The launched processes of forestry transformation began to have a negative impact. On the other hand, in 2012, there were massive forest fires in the Tomsk region [71], including the territory of the Tomsk agglomeration. Logging residues, landfills and windfall as a result of these forest fires burned out to a large extent in that year. Figure 5e shows that by 2020, forest fragmentation has increased again. This is due to the implementation in 2014 of economic sanctions against the Russian Federation. This led to a decrease in the standard of living of the population [72]. The marginal part of the population, especially the rural one, again began to practice illegal logging and ignore garbage disposal. Figure 5f shows that these processes have intensified even more. It can be assumed that, on the one hand, this is due to the decline in the economy due to the coronavirus pandemic [73]. On the other hand, in 2022, the sanctions pressure on the Russian Federation was unprecedentedly increased.

An analysis of the area of urban areas (territories with a population) shows a gradual reduction in these areas from 1990 until the present. Along with the collapse of the Soviet Union in the Russian Federation, there was a destruction of agriculture. As a result of these negative processes, there was an outflow of the population from rural areas to large cities of the Tomsk agglomeration, such as Tomsk and Seversk.

The dynamics of vegetation in the Tomsk agglomeration is shown in the Table 5. The area occupied by vegetation increased from 1990 to 2013. This is especially noticeable in the southern part of the territory, where there is an overgrowth of empty territories.

Table 5. Vegetation dynamics from 1990–2022 in the Tomsk agglomeration.

Year	Vegetation Area, km ²
1990	9758.949
1999	9324.871
2007	10,650.63
2013	11,137.16
2020	10,108.4
2022	10,011.07

The dynamics of changes in the territories covered with vegetation can be traced in the results obtained. Nevertheless, it should be noted that when using optical images, it is difficult to separate the territory of bare soils from technogenic territories (Figure 6). They have a close spectral response and, accordingly, do not align with indices [74]. The use of additional radar survey data should help in solving this problem, since it will allow us to

take into account the heterogeneity of the surface. Additionally, the use of a more frequent time series will allow us to determine the most “cloudless years” and use these data for analysis. The assessment of the accuracy of the results at this stage of the work was carried out visually using a topographic map of the area.

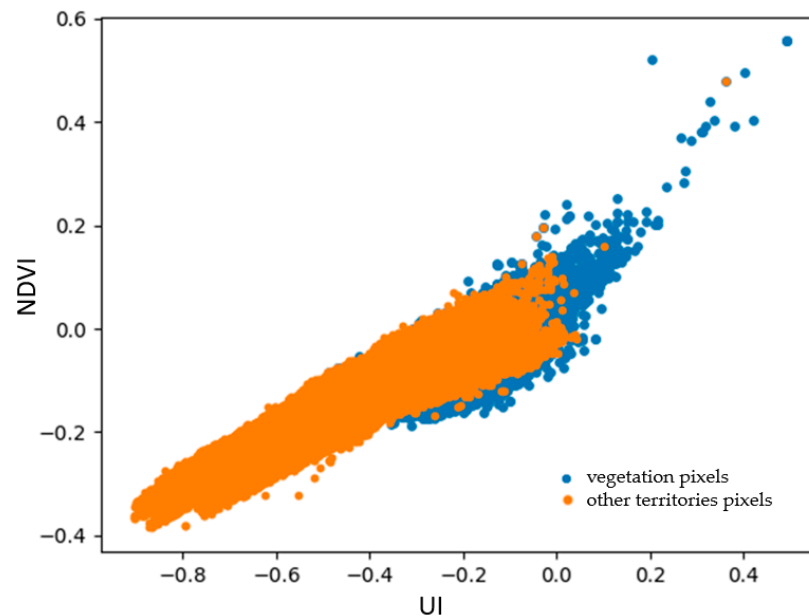


Figure 6. Scatter plots of land cover types in the Tomsk agglomeration in the spectral space of NDVI and UI.

It should be noted that a pilot study of the territory of the Tomsk agglomeration was carried out. In the future, the study area should be extended at the first stage to the entire territory of the Tomsk region [75]. At the second stage, the territory of the Siberian Federal District should be considered. At the last stage, a similar study should be carried out on the scale of the territory of the entire the Russian Federation. In addition, future studies should involve data from the MODIS Terra/Aqua [76] and Sentinel-2A [77] satellite systems to analyze the fire component of vegetation transformation processes within the Tomsk agglomeration and larger territories of the Russian Federation.

Moreover, the study has some limitations, which should be discussed separately. First, forested areas are considered in general, without distinguishing coniferous, deciduous and mixed forests, as well as herbaceous vegetation. In the future, it would be logical to conduct a study with the differentiation of forested areas. Secondly, when analyzing satellite data, such linear sources of anthropogenic load as the railway, roads and riverbeds were not analyzed [78,79]. Accounting for these objects could contribute to a more accurate explanation of changes in the forest area of the territory of the Tomsk agglomeration. Thirdly, as already mentioned, it is necessary to take into account at least MODIS Terra/Aqua satellite data. At the moment, they have not been used. A joint analysis of data on thermal anomalies could support a number of arguments in favor of the announced mechanisms for the transformation of the forest massif of the Tomsk agglomeration.

Furthermore, own unique software for analyzing satellite data was developed as a result of the study. No commercial packages have been used for these purposes. This may allow the developed software to be put into operation in the future as part of the Information System for Remote Monitoring of Forest Fires, ISDM-Rosleskhoz [80]. The operator of this system is Avialesookhrana of the Russian Federation. The ISDM-Rosleskhoz system allows you to analyze information on the territory of the entire Russian Federation. In the future, the modernization of ISDM-Rosleskhoz using the program code developed in the framework of this study can help improve the quality of planning and forestry management in the Russian Federation.

The algorithm for analyzing the dynamics of the area of forest vegetation is implemented in Python. The script uses Rasterio and Fiona tools [81,82]. It allows you to automatically select prepared satellite images and the boundaries of the study area. Landsat input data and a territory boundary vector file were used for the scenario. When you run the tool, you are asked for the path to the spacemen and to the borders file. As a result of the script execution, thematic maps were created, which show the spatial distribution of vegetation from 1990 to 2022. A comparison of the obtained results makes it possible to trace the change in time and space in the area of vegetation. Maps with generalized results of the performed space-time analysis within the Tomsk agglomeration are presented. The developed methodology and algorithm for working with Landsat satellite images provide an opportunity to assess the state and dynamics of spatial and temporal changes in the vegetation cover in the study area.

The second aspect related to the novelty of the study should be considered. In addition to the technological novelty associated with the development of its own program code, the results of the study are new in the context of assessing changes in the forest cover of the Tomsk agglomeration under the influence of local, domestic and external social, economic and political factors. The vast majority of scientific studies on the application of remote sensing are regional studies. Such results, of course, cannot be extrapolated to other territories. However, this is their novelty, value and uniqueness in obtaining new knowledge about the processes taking place in such territories. It should be noted that in the Russian Federation, no one has assessed changes in forest cover with their linkage to social, environmental and political processes in the country and the world. It would be erroneous to link changes in the forest cover of urban agglomerations only with climatic and weather changes, forest successions within the forest biogeocenosis. This article reveals the patterns of changes in forest cover in the Tomsk agglomeration in their connection with economic, social and political processes. This is the second aspect of the novelty of the study. The choice of the territory of the Tomsk agglomeration is not accidental. The most significant climatic changes occur in Western Siberia [73], where the Tomsk agglomeration is located. Therefore, the study of changes in forest cover in this area in the context of social, economic and political factors is of particular importance. It is remote sensing technologies that make it possible to determine these changes.

6. Conclusions

The first study of the territory of the Tomsk agglomeration was carried out. In the future, the study area should be extended to larger territories of the Russian Federation, including the entire territory of the state. In addition, future studies should involve data from the MODIS Terra/Aqua and Sentinel-2A satellite systems to analyze the fire component of vegetation transformation processes within the Tomsk agglomeration and larger territories of the Russian Federation.

Key results and conclusions:

(1) The area of non-forested areas increased from 1990 to 1999 and from 2013 to 2022. It is very likely that this is due to the deterioration of the standard of living in the country during these periods. The first time interval corresponds to the post-Soviet period and the devastation in the economy in the 1990s. The second period corresponds to the implementation and strengthening of sanctions pressure on the Russian Federation.

(2) The area of territories inhabited by people has been steadily falling since 1990. This is due to the destruction of collective agriculture in the Russian Federation and the outflow of the population from the surrounding rural settlements to Tomsk and Seversk.

The development of unique software will make it possible to put it into operation in the foreseeable future as part of the Information System for Remote Monitoring of Forest Fires ISDM-Rosleskhoz. In the future, this will contribute to improving the quality of planning and forestry management in the Russian Federation.

In the future, the study area should be extended at the first stage to the entire territory of the Tomsk region. At the second stage, the territory of the Siberian Federal District

should be considered. At the last stage, a similar study should be carried out on the scale of the territory of the entire Russian Federation. In addition, future studies should involve data from the MODIS Terra/Aqua and Sentinel-2A satellite systems to analyze the fire component of vegetation transformation processes within the Tomsk agglomeration and larger territories of the Russian Federation. Moreover, separate vegetation types will be analyzed within the future researches.

Author Contributions: Conceptualization, E.P.Y., K.S.Y. and N.V.B.; methodology, E.P.Y., K.S.Y. and N.V.B.; software, E.P.Y. and K.S.Y.; validation, E.P.Y. and K.S.Y.; formal analysis, E.P.Y., K.S.Y. and N.V.B.; investigation, E.P.Y., K.S.Y. and N.V.B.; resources, E.P.Y. and K.S.Y.; data curation, E.P.Y. and K.S.Y.; writing—original draft preparation, E.P.Y., K.S.Y. and N.V.B.; writing—review and editing, E.P.Y., K.S.Y. and N.V.B.; visualization, E.P.Y. and K.S.Y.; supervision, N.V.B.; project administration, E.P.Y. and N.V.B. All authors have read and agreed to the published version of the manuscript.

Funding: This research received no external funding.

Data Availability Statement: Data can be requested from authors.

Conflicts of Interest: The authors declare no conflict of interest.

References

- Jingyi Yang, J.; Wang, Z.; Pan, Y. Shifts in plant ecological strategies in remnant forest patches along urbanization gradients. *For. Ecol. Manag.* **2022**, *524*, 120540. [CrossRef]
- Veselkin, D.V. Urbanization increases the range, but not the depth, of forest edge influences on *Pinus sylvestris* bark pH. *Urban For. Urban Greening* **2022**, *79*, 127819. [CrossRef]
- Mitchell, M.G.E.; Devisscher, T. Strong relationships between urbanization, landscape structure, and ecosystem service multifunctionality in urban forest fragments. *Landsc. Urban Plan.* **2022**, *228*, 104548. [CrossRef]
- Chen, X.; Zhang, X.; Wei, H. Urbanization induced changes in the accumulation mode of organic carbon in the surface soil of subtropical forests. *CATENA* **2022**, *214*, 106264. [CrossRef]
- Vacca, P.; Caballero, D.; Planas, E. WUI fire risk mitigation in Europe: A performance-based design approach at home-owner level. *J. Saf. Sci. Resil.* **2020**, *1*, 97–105. [CrossRef]
- Vaiculyte, S.; Hulse, L.M.; Veeraswamy, A. Exploring ‘wait and see’ responses in French and Australian WUI wildfire emergencies. *Saf. Sci.* **2022**, *155*, 105866. [CrossRef]
- Hysa, A. Indexing the vegetated surfaces within WUI by their wildfire ignition and spreading capacity, a comparative case from developing metropolitan areas. *Int. J. Disaster Risk Reduct.* **2021**, *63*, 102434. [CrossRef]
- Pohjola, J.; Turunen, J.; Ikonen, A.T.K. On the inclusion of forest exposure pathways into a stylized lake-farm scenario in a geological repository safety analysis. *J. Environ. Radioact.* **2022**, *255*, 107019. [CrossRef]
- Ahmadvand, S.; Khadivi, M.; Sowlati, T. Bi-objective optimization of forest-based biomass supply chains for minimization of costs and deviations from safety stock. *Energy Convers. Manag.* **2021**, *11*, 100101. [CrossRef]
- Unver, S.; Ergenc, I. Safety risk identification and prioritize of forest logging activities using analytic hierarchy process (AHP). *Alex. Eng. J.* **2020**, *60*, 1591–1599. [CrossRef]
- Barta, K.A.; Hais, M.; Heurich, M. Characterizing forest disturbance and recovery with thermal trajectories derived from Landsat time series data. *Remote Sens. Environ.* **2022**, *282*, 113274. [CrossRef]
- Viana-Soto, A.; Okujeni, A.; Hostert, P. Quantifying post-fire shifts in woody-vegetation cover composition in Mediterranean pine forests using Landsat time series and regression-based unmixing. *Remote Sens. Environ.* **2022**, *281*, 113239. [CrossRef]
- Maeda, E.E.; Formaggio, A.R.; Hansen, M.C. Predicting forest fire in the Brazilian Amazon using MODIS imagery and artificial neural networks. *Int. J. Appl. Earth Obs. Geoinf.* **2009**, *11*, 265–272. [CrossRef]
- Silveira, E.M.O.; Radeloff, V.C.; Pidgeon, A.M. Nationwide native forest structure maps for Argentina based on forest inventory data, SAR Sentinel-1 and vegetation metrics from Sentinel-2 imagery. *Remote Sens. Environ.* **2022**, *285*, 113391. [CrossRef]
- Eskandari, S.; Sarab, S.A.M. Mapping land cover and forest density in Zagros forests of Khuzestan province in Iran: A study based on Sentinel-2, Google Earth and field data. *Ecol. Inform.* **2022**, *70*, 101727. [CrossRef]
- Do-Hyung, K.; Joseph, O.; Sexton, P.N.; Chengquan, H.; AnupamAnand, S.C.; Feng, M.; John, R. Townshend Global, Landsat-based forest-cover change from 1990 to 2000. *Remote Sens. Environ.* **2014**, *155*, 178–193.
- Yankovich, K.S.; Yankovich, E.P.; Baranovskiy, N.V. Classification of Vegetation to Estimate Forest Fire Danger Using Landsat 8 Images: Case Study (2019). *Math. Probl. Eng.* **2019**, 6296417. [CrossRef]
- Baranovskiy, N.V.; Yankovich, K.S.; Yankovich, E.P. Preliminary estimation of forest fire danger using LANDSAT images over Baikal Lake basin forests (2018). In Proceedings of the 24th International Symposium on Atmospheric and Ocean Optics: Atmospheric Physics, Tomsk, Russian, 13 December 2018; p. 10833.

19. Zhou, X.; Hao, Y.; Di, L.; Wang, X.; Chen, C.; Chen, Y.; Nagy, G.; Jancso, T. Improving GEDI Forest Canopy Height Products by Considering the Stand Age Factor Derived from Time-Series Remote Sensing Images: A Case Study in Fujian, China. *Remote Sens.* **2023**, *15*, 467. [CrossRef]
20. Shamsuzzoha, M.; Ahamed, T. Shoreline Change Assessment in the Coastal Region of Bangladesh Delta Using Tasseled Cap Transformation from Satellite Remote Sensing Dataset. *Remote Sens.* **2023**, *15*, 295. [CrossRef]
21. Ullah, W.; Ahmad, K.; Ullah, S.; Tahir, A.A.; Javed, M.F.; Nazir, A.; Abbasi, A.M.; Aziz, M.; Mohamed, A. Analysis of the relationship among land surface temperature (LST), land use land cover (LULC), and normalized difference vegetation index (NDVI) with topographic elements in the lower Himalayan region. *Heliyon* **2023**, *9*, e13322. [CrossRef]
22. ENVI—Image Processing and Analysis Software Solution. Available online: <https://www.itervis.com/envi/> (accessed on 14 January 2023).
23. ScanEx Image Processor. Available online: <https://www.scanex.ru/software/obrabotka-izobrazheniy/scanex-image-processor/> (accessed on 14 January 2023).
24. SARproZ. Available online: <https://www.scanex.ru/software/obrabotka-izobrazheniy/sarproz/> (accessed on 14 January 2023).
25. Python. Available online: <https://www.python.org/> (accessed on 14 January 2023).
26. Michael, A.; Wulder, J.C.; White, S.N.; Goward, J.G.; Masek, J.R.; Irons, M.H.; Warren, B.; Cohen, T.R.; Loveland, C.E. Woodcock, Landsat continuity: Issues and opportunities for land cover monitoring. *Remote Sens. Environ.* **2008**, *112*, 955–969. [CrossRef]
27. Landsat Satellite Missions. Available online: <https://www.usgs.gov/landsat-missions/landsat-satellite-missions> (accessed on 27 December 2022).
28. Michael, A.; Wulder, D.P.; Roy, V.C.; Radeloff, T.R.; Loveland, M.C.; Anderson, D.M.; Johnson, S.H.; Zhu, Z.; Theodore, A.; Scambos, N.P.; et al. Cook, Fifty years of Landsat science and impacts. *Remote Sens. Environ.* **2022**, *280*, 113195. [CrossRef]
29. Landsat Collection 2. Available online: <https://www.usgs.gov/landsat-missions/landsat-collection-2> (accessed on 27 December 2022).
30. Phiri, D.; Simwanda, M.; Salekin, S.; Nyirenda, V.R.; Murayama, Y.; Ranagalage, M. Sentinel-2 Data for Land Cover/Use Mapping: A Review. *Remote Sens.* **2020**, *12*, 2291. [CrossRef]
31. Morell-Monzó, S.; Estornell, J.; Sebastiá-Frasquet, M.-T. Comparison of Sentinel-2 and High-Resolution Imagery for Mapping Land Abandonment in Fragmented Areas. *Remote Sens.* **2020**, *12*, 2062. [CrossRef]
32. Dara, A.; Baumann, M.; Kuemmerle, T.; Pflugmacher, D.; Rabe, A.; Griffiths, P.; Hölzel, N.; Kamp, J.; Freitag, M.; Hostert, P. Mapping the timing of cropland abandonment and recultivation in northern Kazakhstan using annual Landsat time series. *Remote Sens. Environ.* **2018**, *213*, 49–60. [CrossRef]
33. Müller, D.; Leitão, P.J.; Sikor, T. Comparing the determinants of cropland abandonment in Albania and Romania using boosted regression trees. *Agric. Syst.* **2013**, *117*, 66–77. [CrossRef]
34. Yin, H.; Prishchepov, A.V.; Kuemmerle, T.; Bleyhl, B.; Buchner, J.; Radeloff, V.C. Mapping agricultural land abandonment from spatial and temporal segmentation of Landsat time series. *Remote Sens. Environ.* **2018**, *210*, 12–24. [CrossRef]
35. Kuemmerle, T.; Hostert, P.; Radeloff, V.C.; Linden, S.; Perzanowski, K.; Kruhlov, I. Cross-border Comparison of Post-socialist Farmland Abandonment in the Carpathians. *Ecosystems* **2008**, *11*, 614–628. [CrossRef]
36. Grădinaru, S.R.; Kienast, F.; Psomas, A. Using multi-seasonal Landsat imagery for rapid identification of abandoned land in areas affected by urban sprawl. *Ecol. Indic.* **2019**, *96*, 79–86. [CrossRef]
37. Prishchepov, A.V.; Radeloff, V.C.; Dubinin, M.; Alcántara, C. The effect of Landsat ETM/ETM image acquisition dates on the detection of agricultural land abandonment in Eastern Europe. *Remote Sens. Environ.* **2012**, *126*, 195–209. [CrossRef]
38. Baumann, M.; Kuemmerle, T.; Elbakidze, M.; Ozdogan, M.; Radeloff, V.C.; Keuler, N.S.; Prishchepov, A.V.; Kruhlov, I.; Hostert, P. Patterns and drivers of post-socialist farmland abandonment in Western Ukraine. *Land Use Policy* **2011**, *28*, 552–562. [CrossRef]
39. Koroleva, N.V.; Tihonova, E.V.; Ershov, D.V.; Saltykov, A.N.; Gavriljuk, E.A.; Pugachevskij, A.V. Ocenka masshtabov zarastaniya nelesnyh zemel' v nacional'nom parke "Smolenskoe poozer'e" za 25 let po sputnikovym dannym Landsat (Assessment of the extent of non-forest lands growing in the Smolensk Lakeland National Park for 25 years using satellite data Landsat). *Lesovedenie* **2018**, *2*, 83–96.
40. Phiri, D.; Morgenroth, J. Developments in Landsat Land Cover Classification Methods: A Review. *Remote Sens.* **2017**, *9*, 967. [CrossRef]
41. Schowengerdt, R.A. *Techniques for Image Processing and Classifications in Remote Sensing*; Academic Press: Cambridge, MA, USA, 2012.
42. Potapov, P.; Turubanova, S.; Matthew, C. Hansen, Regional-scale boreal forest cover and change mapping using Landsat data composites for European Russia. *Remote Sens. Environ.* **2011**, *115*, 548–561. [CrossRef]
43. Campbell, J.B.; Wynne, R.H. *Introduction to Remote Sensing*; Guilford Press: New York, NY, USA, 2011; Volume 5.
44. Lu, D.; Weng, Q. A survey of image classification methods and techniques for improving classification performance. *Int. J. Remote Sens.* **2007**, *28*, 823–870. [CrossRef]
45. Coppin, P.; Jonckheere, I.K.; Nackaerts, B.; Muys, E. Lambin Review Digital change detection methods in ecosystem monitoring: A review. *Int. J. Remote Sens.* **2004**, *25*, 1565–1596. [CrossRef]
46. Yepintsev, S.A.; Klepikov, O.V.; Shekoyan, S.V. Remote sensing of the Earth as a method of assessing environmental quality of urban areas. *Zdo rov'e Naseleniya i Sreda. Obitalniya* **2020**, *4*, 5–12. [CrossRef]

47. Guindon, B.; Zhang, Y.; Dillabaugh, C. Landsat urban mapping based on a combined spectral–spatial methodology. *Remote Sens. Environ.* **2004**, *92*, 218–232. [[CrossRef](#)]
48. Masek, J.G.; Lindsay, F.E.; Goward, S.N. Dynamics of urban growth in the Washington DC Metropolitan Area, 1973–1996, from Landsat observations. *Int. J. Remote Sens.* **2000**, *21*, 3473–3486. [[CrossRef](#)]
49. Chai, B.; Li, P. An ensemble method for monitoring land cover changes in urban areas using dense Landsat time series data. *ISPRS J. Photogramm. Remote Sens.* **2023**, *195*, 29–42. [[CrossRef](#)]
50. Schneider, A. Monitoring land cover change in urban and peri-urban areas using dense time stacks of Landsat satellite data and a data mining approach. *Remote Sens. Environ.* **2012**, *124*, 689–704. [[CrossRef](#)]
51. Czekajlo, A.; Nicholas, C.; Coops, M.A.; Wulder, T.H.; Joanne, C. Matilda van den Bosch, W. Mapping dynamic peri-urban land use transitions across Canada using Landsat time series: Spatial and temporal trends and associations with socio-demographic factors. *Computers Environ. Urban Syst.* **2021**, *88*, 101653. [[CrossRef](#)]
52. Zha, Y.; Gao, J.; Ni, S. Use of normalized difference built-up index in automatically mapping urban areas from TM imagery. *Int. J. Remote Sens.* **2003**, *24*, 583–594. [[CrossRef](#)]
53. Ridd, M.K. Exploring a V-I-S (vegetation-impervious surface-soil) model for urban ecosystem analysis through remote sensing: Comparative anatomy for cities. *Int. J. Remote Sens.* **1995**, *16*, 2165–2185. [[CrossRef](#)]
54. Curtis, E.; Woodcock, T.R.; Loveland, M.H.; Bauer, M.E. Transitioning from change detection to monitoring with remote sensing: A paradigm shift. *Remote Sens. Environ.* **2020**, *238*, 111558. [[CrossRef](#)]
55. Draft Scheme of Territorial Planning of the Tomsk Region. Explanatory Note. Volume 1 “Regulations on Territorial Planning”. Available online: <https://tomsk.gov.ru/tomskaja-aglomeratsija> (accessed on 15 December 2022). (In Russian)
56. Dyukarev, A.G.; Pologova, N.N.; Lapshina, E.D. *Natural Resource Zoning of the Tomsk Region*; Spektr Publishing House: Tomsk, Russia, 1997; p. 40.
57. Evseeva, N.S. *Geography of the Tomsk Region. (Natural Conditions and Resources)*; Publishing House of Tomsk University: Tomsk, Russia, 2001; p. 223.
58. USGS. Available online: <https://earthexplorer.usgs.gov/> (accessed on 14 January 2023).
59. Elmore, A.; Mustard, J.F.; Manning, S.J.; Lobell, D.B. Quantifying vegetation change in semiarid Environments: Precision and accuracy of spectral mixture analysis and the Normalized Difference Vegetation Index. *Remote Sens. Environ.* **2000**, *73*, 87–102. [[CrossRef](#)]
60. Howard, J.A. *Remote Sensing of Forest Resources: Theory and Application*; Chapman & Hall: New York, NY, USA, 1991; p. 420.
61. Rouse, J.W.; Haas, R.H.; Schell, J.A.; Deering, D.W. Monitoring vegetation systems in the Great Plains with ERTS. *Third ERTS Symp. NASA* **1973**, *351*, 309–317.
62. Gao, B.C. NDWI—A Normalized Difference Water Index for Remote Sensing of Vegetation Liquid Water from Space. *Remote Sens. Environ.* **1996**, *58*, 257–266. [[CrossRef](#)]
63. McFeeters, S.K. The use of the normalized difference water index (NDWI) in the delineation of open water features. *Int. J. Remote Sens.* **1996**, *17*, 1425–1432. [[CrossRef](#)]
64. Kawamura, M.; Jayamana, S.; Tsujiko, Y. Relation between social and environmental conditions in Colombo Sri Lanka and the urban index estimated by satellite remote sensing data. *Int. Arch. Photogramm. Remote Sens.* **1996**, *31*, 321–326.
65. Kawamura, M.; Jayamanna, S.; Tsujiko, Y. Quantitative evaluation of urbanization in developing countries using satellite data. *J. Environ. Syst. Eng.* **1997**, *580*, 45–54. [[CrossRef](#)] [[PubMed](#)]
66. Kawamura, M.; Jayamanna, S.; Tsujiko, Y.; Sugiyama, A. Comparison of urbanization of four Asian cities using satellite data. *J. Environ. Syst. Eng.* **1998**, *608*, 97–105. [[CrossRef](#)] [[PubMed](#)]
67. Available online: <https://landsat.usgs.gov/landsat-8-l8-data-users-handbook> (accessed on 27 December 2022).
68. Abdelal, R. *National Purpose in the World Economy: Post-Soviet States in Comparative Perspective*; Cornell University Press: Ithaca, NY, USA, 2005.
69. Kot, V.; Barsukova, A.; Strielkowski, W.; Krivko, M.; Smutka, L. International Trade in the Post-Soviet Space: Trends, Threats, and Prospects for the Internal Trade within the Eurasian Economic Union. *J. Risk Financ. Manag.* **2023**, *16*, 16. [[CrossRef](#)]
70. Forest Code of the Russian Federation of December 4, 2006 N 200-FZ (LK RF) (as amended). Available online: <https://base.garant.ru/77707148/> (accessed on 14 January 2023).
71. Kuznetsov, G.V.; Baranovskiy, N.V. Focused sun’s rays and forest fire danger: New concept (2013) Proceedings of SPIE. *Int. Soc. Opt. Eng.* **2013**, *8890*, 889011.
72. Bazarova, O.; Bazarov, A.; Baranovskiy, N.; Sychev, R.; Atutov, E. Impact of Population Income on the Number of Forest Fires: A Case Study. *Int. Rev. Model. Simul.* **2022**, *15*, 36–46. [[CrossRef](#)]
73. Rehman, A.U.; Mian, S.H.; Usmani, Y.S.; Abidi, M.H.; Mohammed, M.K. Modeling Consequences of COVID-19 and Assessing Its Epidemiological Parameters: A System Dynamics Approach. *Healthcare* **2023**, *11*, 260. [[CrossRef](#)]
74. Ettehadi Osgouei, P.; Kaya, S.; Sertel, E.; Alganci, U. Separating Built-Up Areas from Bare Land in Mediterranean Cities Using Sentinel-2A Imagery. *Remote Sens.* **2019**, *11*, 345. [[CrossRef](#)]
75. Baranovskiy, N.V.; Karanina, S.Y.; Kocheeva, N.A.; Belikova, M.Y. Lightning discharges distribution estimation over the Tomsk region in 2010–2015 Proceedings of SPIE. *Int. Soc. Opt. Eng.* **2018**, *10833*, 108337S.
76. Buramuge, V.A.; Ribeiro, N.S.; Olsson, L.; Bandeira, R.R.; Lisboa, S.N. Tree Species Composition and Diversity in Fire-Affected Areas of Miombo Woodlands, Central Mozambique. *Fire* **2023**, *6*, 26. [[CrossRef](#)]

77. Amroussia, M.; Viedma, O.; Achour, H.; Abbes, C. Predicting Spatially Explicit Composite Burn Index (CBI) from Different Spectral Indices Derived from Sentinel 2A: A Case of Study in Tunisia. *Remote Sens.* **2023**, *15*, 335. [CrossRef]
78. Baranovskiy, N. A simplified mathematical model for estimating the anthropogenic load on forest areas in the context of forest fires. *Int. Multidiscip. Sci. GeoConference Surv. Geol. Min. Ecol. Manag.* **2019**, *19*, 723–730.
79. Baranovskiy, N.V.; Ignateva, A.V. Mathematical Modeling of Human Activity on Forested Areas from Point Objects of Railway Infrastructure in a Two-Dimensional Statement. *Int. J. Eng. Appl.* **2022**, *10*, 15–28. [CrossRef]
80. Podolskaya, A.S.; Ershov, D.V.; Shulyak, P.P. Application of the method for assessing the likelihood of forest fires in ISDM-Rosleskhoz. *Mod. Probl. Remote Sens. Earth Space* **2011**, *8*, 118–126.
81. Rasterio Python Tool. Available online: <https://pypi.org/project/rasterio/> (accessed on 8 February 2023).
82. Fiona Python Tool. Available online: <https://pypi.org/project/Fiona/> (accessed on 8 February 2023).

Disclaimer/Publisher’s Note: The statements, opinions and data contained in all publications are solely those of the individual author(s) and contributor(s) and not of MDPI and/or the editor(s). MDPI and/or the editor(s) disclaim responsibility for any injury to people or property resulting from any ideas, methods, instructions or products referred to in the content.